

Tsunami Forecasting and Risk Assessment

New Mexico

Supercomputing Challenge

Final Report

April 3, 2019

Team Number 97

Los Alamos High School

Team Members:

Robert R. Strauss

Logan B. Dare

Teachers:

Mark Petersen

Project Mentor:

Charlie E. M. Strauss

Table of Contents

1 Executive Summary	3
2 Introduction	4
Palu.....	4
What was different this time in Palu?	4
Krakatoa	5
Why Krakatoa?.....	6
Scaling the computational model	6
Roadmap of this report	6
3 Methods	7
The physics.....	7
Finite element grid.....	8
Time step propagation	8
Numerical stability resolved.....	8
Data sets and management.....	9
From single threaded to massively parallel vector computation.....	9
Refinement & Verification	9
4 Results	11
Palu	11
Krakatoa	14
Computer Model	14
5 Discussion	18
Palu	18
Did the harbor shape or bathymetry have an effect?	18
Did the tsunami's initial location have an effect?	18
Did the properties of the wave have an effect?	18
Krakatoa	19
6 Conclusion	21
7 Acknowledgements	21
8 References	22

1 Executive Summary

Tsunamis are tragic events, killing thousands of people at a time, and to make matters worse, they often come unexpectedly because they affect places far from the point of origin. Two tsunamis have struck in Indonesia alone in the past six months, together killing over a thousand people. Can the damage from a tsunami be forecasted? Tsunamis can be simulated on supercomputers, but this is clearly not effective for real-time warning; if it were, the death count in each of these events would be much lower. I created a faster than real-time, highly accurate, and very affordable computer-based tsunami forecasting system, that has the potential to be part of a life-saving early warning system.

I built my model by creating a finite-element implementation of a set of differential equations. I numerically solved the non-linear coupled partial shallow water equations, describing the interaction between sea surface height and water velocity. I constructed a computer program including differential functions, time-step integrators, unit tests, and data and results visualization in thousands of lines of code, all from scratch. My model was my own creation; I did not implement a pre-existing ocean simulation engine. This meant I could write my code in a way that allowed for parallelization to run on a computer graphics card. This both cuts down the price dramatically from that of a supercomputer, while accelerating the simulation speed of my model to 28 times faster than real time. This makes it affordable to agencies of developing countries or even small villages.

I validated my forecasting system on the outcomes of two real tsunamis that happened last year: a tsunami that devastated Palu City, Indonesia, and one triggered by the eruption of volcano Anak Krakatoa. The destruction to Palu was surprising because Palu seemed to be protected from previous tsunamis by its harbor. To determine the factors contributing to the severity of this case, I asked three questions: First, “did the harbor shape or ocean floor topology have an effect”, second, “did the initial location of the wave have an effect”, and third, “did the properties of the wave have an effect”. I simulated several tsunami events with my model to answer these. I answered the questions I asked, and in doing so I isolated the key factors in the severity of the Palu case. For the Krakatoa tsunami, I tested the accuracy of my model at predicting the distribution of damage from a tsunami. I simulated the Krakatoa tsunami, and compared the forecasted damage from my model to the real damage. I found that my model accurately predicted not only hazard areas but safe zones. My tool has a user interface, simulates significantly faster than real time, and is connected to a database allowing it to be applied to any area on Earth.

2 Introduction

Seismic events such as landslides and earthquakes near water create tsunamis, whose impact can be devastating and deadly. Tsunamis can deliver immense damage at places far from their origin and often arrive without warning. Risk analysis of coastal areas can be aided by computational modeling of tsunamis. In a computer model, the initial conditions and factors can be altered, whereas there is only one data point from real life. Thus a computer model is especially useful for risk assessment. This project produced a computer model with an easily adjusted user interface that also presents results with graphs, heat maps, and animations.

Simulation also allows multiple types of assessment. One type is to start hypothetical tsunamis at likely points of origin, such as an earthquake fault, then predict the resulting distribution of damage to surrounding coasts. Another type is to investigate why, that is what special features, put certain coastal regions at higher risk than others. Here, both types of assessment are demonstrated in the context of the 2018 Palu earthquake-tsunami and the 2019 Anak Krakatoa volcano landslide-tsunami.

Palu

In 2018 a tsunami devastated Palu city, Indonesia.

- More than 800 people were killed.
- Over 500 were severely injured.
- 48,000 were made homeless

The Palu region is shown in figure 1. Before and after images of a bridge in Palu to give a sense of the extreme power of the impact. (Figure 2 and figure 3)

What was different this time in Palu?

Palu is deep inside a protective harbor. Historically, it had been a rather safe area from tsunamis, so it was especially surprising this tsunami devastated Palu to the extent that it did. Media speculations included the shape of the harbor guiding the wave or the special location of the tsunami or the direction or type of the earthquake fault making for enhanced severity. (4,5)

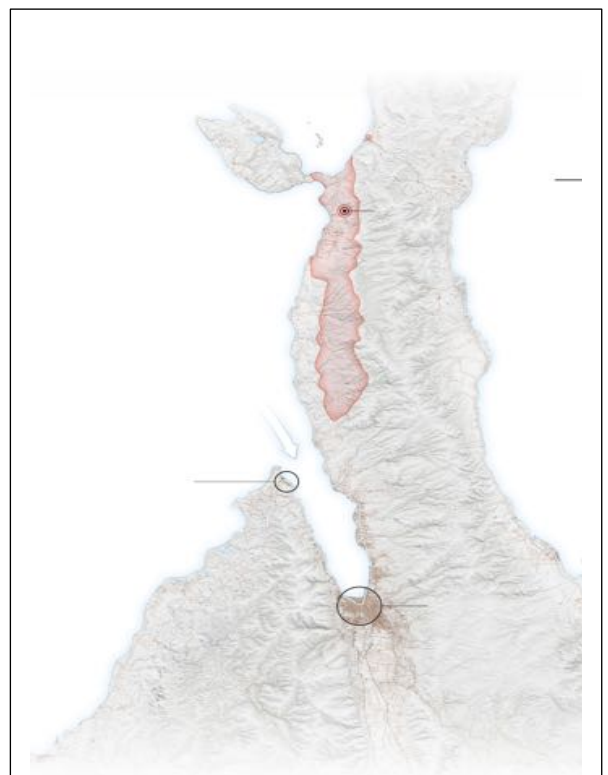


Figure 1: (NY Times) Map around Palu, Indonesia, showing earthquake epicenter (red dot), area of most intense earthquake shaking (red area), and damage to Palu (shaded in brown). Up is North.



Figure 2: (NY Times) Bridge in Palu before tsunami. In good condition, undamaged.



Figure 3: (NY Times) The same bridge after the tsunami completely destroyed

All of these factors are plausible, but what contributes most to the severity? I asked three questions: “did the harbor shape or ocean floorTo answer this, the effect of the tsunami at Palu is observed as I change its initial parameters including its point of origin, type of wave, and angle. Furthermore, I looked at a time series of the tsunami’s evolution in the harbor channel to see how the bathymetry profile (ocean topology/depth) contributed to the severity.

I found that the location of the tsunami was critical to admit wave energy into the harbor. But once in the harbor, the location of the damage was determined by the bathymetry more than the point of origin. Additionally, the shape and direction of the wave had only minor effect. While the guesses in the media were obvious ones to make, not all of them were correct and the results depended on the unfortunate combination of factors. *For example, if Palu had been located at a different point along the channel it might have evaded much destruction.*

Interestingly, I also discovered that a second completely unexpected mode for strong energy coupling into Palu harbor was possible, greatly enlarging the origin hazard zone. This was from a Kelvin wave being guided along the shore up North to the mouth of Palu bay (“Kelvin Waves”). A Kelvin wave is a phenomenon that occurs when the Coriolis force – a fictitious force from the spinning of the Earth – pushes a wave against a bathymetric feature, and between the two the wave is guided in a direction. I observe in both the wave patterns and maximum height predictions that it can, surprisingly, round the corner and enter into the harbor, despite the point of origin appearing to be blocked by the harbor orientation.

Krakatoa

The second case (figures 4, 5) that was investigated was the collapse of volcano Anak Krakatoa in Indonesia. Anak Krakatoa is in the ocean, so when it collapsed it caused a tsunami. The nearby islands of Java and Sumatra suffered major devastation from this tsunami. In the Krakatoa tsunami: (figures 4,5)

- Over 500 people were killed.
- Over 1400 people were injured.



Figure 4: (The Telegraph) Scene of destruction caused by the Krakatoa tsunami

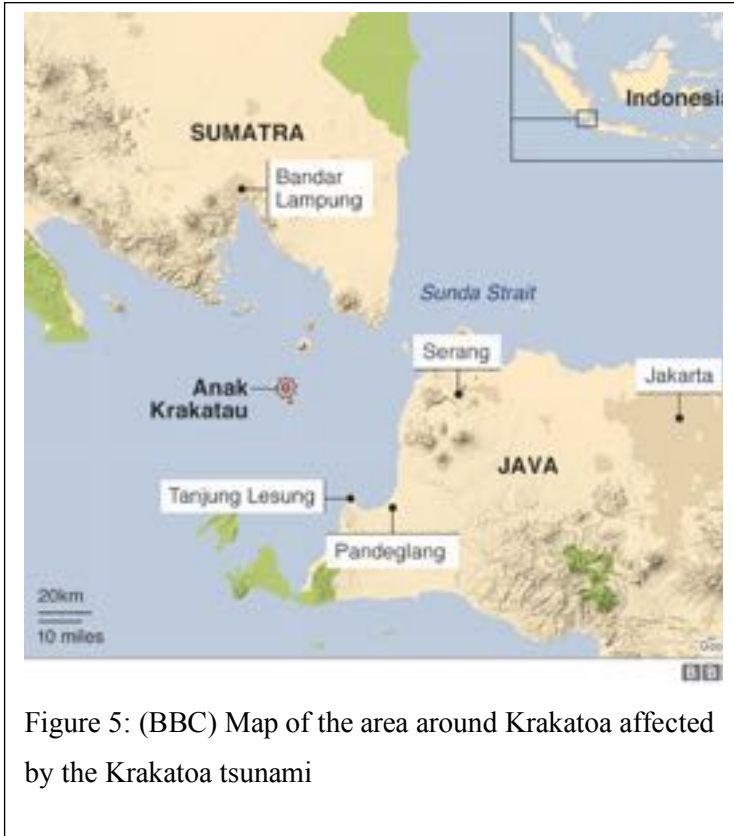


Figure 5: (BBC) Map of the area around Krakatoa affected by the Krakatoa tsunami

Why Krakatoa?

When this project was started, a list of likely tsunami origins that could be simulated to forecast risk regions was compiled. High among these was the infamous Krakatoa volcano tsunami from 1883, the largest tsunami in recorded history, killing tens of thousands of people in diverse and distant areas. Coincidentally, during this project a cinder cone on the caldera of Krakatoa erupted, creating a landslide, which in turn created a tsunami. This is the event that will be forecast in this report. This widened the scope of the project from one of demonstrating a forecast to analyzing the agreement of my model to the actual event.

From the perspective of additional validation, the agreement of the model to the real outcome shows the power of this for risk assessment. No parameters of the simulation were artificially altered to increase agreement, meaning this model was run in a forecasting mode, not a model-fitting mode.

Scaling the computational model

To model larger forecast-scale regions and with higher accuracy, the simulation system was scaled up to use the memory more efficiently as well as speed up the calculations, cutting simulation time down from days to hours. Supercomputing advisors suggested using a large cluster. Instead I initially scaled to eight parallel CPU cores each with four-wide SIMD vector processing. Then I scaled to tens of thousands of threads on thousands of processors with 32-wide SIMD vector processing via a GPU.

Roadmap of this report

This paper is organized as follows: how the simulation was developed is discussed within the methods section. The physics is modeled by Non-linear shallow water differential equations. I discuss how they were implemented computationally, finite element and finite time step discretization, how instabilities were avoided, where bathymetry data was acquired, and more. The implementation is verified. Applications to understanding Palu and forecasting Krakatoa are shown in the results section. The discussion analyzes the data, showing that the forecasts are validated.

Code for this project can be found here: <http://github.com/robertstrauss/shallowwater>

3 Methods

The physics

The approximated physics of the model is entirely contained in a set of coupled partial differential equations, known as the “non-linear shallow water equations” (“Thacker, William Carlisle”), shown in figure 6. There are no adjustable parameters – any coefficients are set constants such as gravity – meaning there is no model fitting aspect in this project. Instead, the experimental parameters of the simulation are event location, coastal boundary condition, and wave shape.

The shallow water equations are an approximation of the behavior of water. In a shallow water equations system, a body of water is simplified to many individual columns of water of varying height and velocity. The equations incorporate terms for advection, a sort of momentum for propagating waves, attenuation, a friction term, and the Coriolis force, a fictitious force arising from the rotation of the Earth.

$$\frac{\partial \eta}{\partial t} = -\frac{\partial}{\partial x}((\eta + h)u) - \frac{\partial}{\partial y}((\eta + h)v)$$

$$\frac{\partial u}{\partial t} = \text{Coriolis} + \text{Advection} + \text{Gravity} + \text{Attenuation}$$

$$= +fv + (\kappa \nabla^2 u - (u, v) \cdot \vec{\nabla} u) - g \frac{\partial \eta}{\partial x} - \frac{1}{\rho(h + \eta)} \mu u \sqrt{u^2 + v^2}$$

$$= +fv + \left(\kappa \frac{\partial^2 u}{\partial x^2} + \kappa \frac{\partial^2 u}{\partial y^2} - u \frac{\partial u}{\partial x} - v \frac{\partial u}{\partial y} \right) - g \frac{\partial \eta}{\partial x} - \frac{1}{\rho(h + \eta)} \mu u \sqrt{u^2 + v^2}$$

$$\frac{\partial v}{\partial t} = -fu + (\kappa \nabla^2 v - (u, v) \cdot \vec{\nabla} v) - g \frac{\partial \eta}{\partial y} - \frac{1}{\rho(h + \eta)} \mu v \sqrt{u^2 + v^2}$$

$$= -fu + \left(\kappa \frac{\partial^2 v}{\partial x^2} + \kappa \frac{\partial^2 v}{\partial y^2} - u \frac{\partial v}{\partial x} - v \frac{\partial v}{\partial y} \right) - g \frac{\partial \eta}{\partial y} - \frac{1}{\rho(h + \eta)} \mu v \sqrt{u^2 + v^2}$$

h - bathymetry (depth)

f - Coriolis force $\propto \sin(\text{latitude})$

η - surface height deviation

κ - viscous damping coefficient

u - X speed (East)

μ - friction coefficient

v - Y speed (North)

g - gravity

Figure 6: The shallow water equations. A set of three differential equations, representing the rate of change of the sea surface height and velocities.

To implement these equations computationally, discretization was performed and a time-step integrator for these equations was constructed from scratch.

Finite element grid

A computer model was created to simulate the ocean. To do this, a system for storing the state of a body of water as well as a finite element model of the shallow water equations (via discretization) had to be engineered. This meant creating a discrete system, in which time and space come in discrete chunks rather than continuously. The size of the time step was determined from the size of spatial elements and the depth. The shallow water equations can be approximated to a simple linear wave equations producing a depth-dependent wave speed, equal to the square root of the product of the depth and the gravitational acceleration ($c = \sqrt{gh}$). The time step ' Δt ' must be shorter than the time it takes for a wave to move across the width of an element, ' Δx '. Thus, Δt and Δx are related by $\Delta t < \Delta x/c$. This is known as the CFL condition (Caminha, Guilherme)

Time step propagation

The shallow water equations give the rate of change of the water height and velocity at each time step. The most obvious approach would be to simply add the rate of change times the timestep on to the values. However, this can be unstable. Several other methods of higher order integration were investigated.

The time-step integrator had multiple time-stepping methods: a simple forward Euler method, a forward-backward method, a forward-backward method with a corrector step (forward-backward feedback), and a generalized forward-backward method. There was a time-memory tradeoff between these time-stepping methods; The generalized forward-backward time-step, for example, was faster than the forward-backward feedback time-step, but took up more memory at a time.

Numerical stability resolved

Finite element simulation of coupled partial differential equations can have stability issues. There are three ways to deal with these. First, a higher order approximation integrator can be used as noted above. Second, the temporal and spatial step sizes can be reduced using the CFL condition. And third, damping can be introduced.

The damping term appears in the equations due to the friction with the ocean floor. However, because the shallow water equations integrate out the entire vertical water column the friction coefficient is affecting the entire finite element water speed. Since setting the coefficient on the damping term seems to be in a way subjective (private communication with Bill Lucy Knight, University of Alaska), it was aimed to set this to be as small as possible. To determine this value, the damping coefficient was slowly increased until the differential equations became stable. In the literature of the Non-linear shallow water equations, the viscosity term appears to be usually ignored because it's a higher order approximation, so

chi (κ) was set to zero. (private communication with Bill Lucy Knight, University of Alaska) This is useful for a second reason: the viscosity term can be numerically unstable since it is a higher order derivative whereas the damping term is stabilizing.

Data sets and management

Bathymetry (ocean depth) data was acquired from The CoNED project (“Coastal National Elevation Database (CoNED) Project - Topobathymetric Digital Elevation Model (TBDEM) | The Long Term Archive”), and packages such as pandas and netCDF were used to query these large data within the program. This allows the program to consider any region of Earth just by inputting the coordinates.

From single threaded to massively parallel vector computation

Computational methods were investigated for optimizing the speed of the code’s execution. The code was implemented with pure python, the slowest method; the numpy python library, allowing for array calculations; the numba library, which compiled the python code; and the cuda library, allowing for the code to be run on the graphics card in a massively parallel way. On a small test case of array size 200 by 200 the time the code took to complete a simulation was recorded: pure python was the slowest method, with a time of 39.9 seconds; numpy was much faster, with a time of 1.0 second; numba was even faster, with a time of 0.4 seconds; and cuda was by far the fastest, with a time of 0.05 seconds, about 800 times faster than pure python.

Scaling up to 200 times to 4000x2000 point arrays and a long 550 second simulation, I observed the cuda ran in 19 seconds and the Numba in 1260 seconds, showing the graphics card gains more as the array size increases (from 8 times faster to 66 times faster).

Refinement & Verification

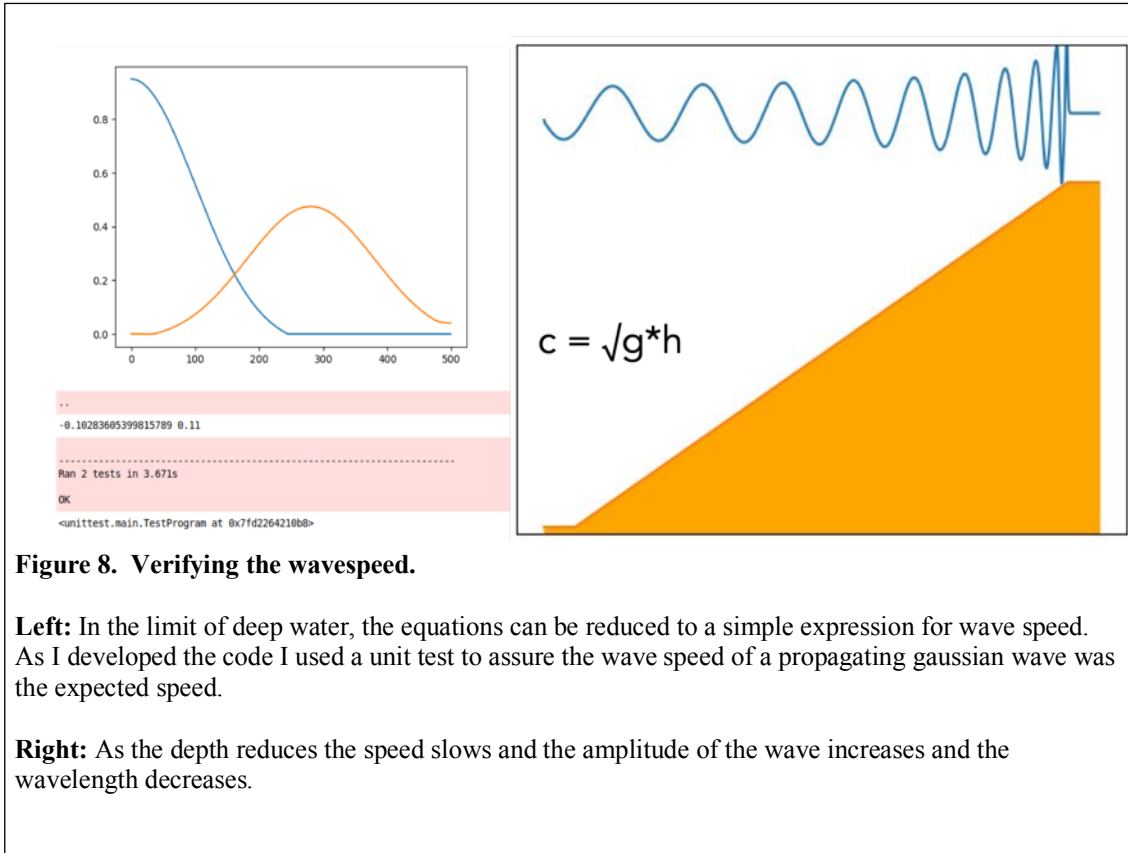
Most of the time in this project was spent developing and refining the model. I began with the forward Euler time-step, but doing larger and longer simulations caused instabilities with that technique, so I switched to a forward-backward predictor-corrector time-step. I also created restrictions in my model to make sure the CFL condition was met. To make sure my model was working correctly, I verified it with unit tests.

Verification is checking that a model is working as expected and not breaking down, while validation is checking if the model is accomplishing the overall goal. The shallow water equations are a well-known and valid model. However, because I created my own new implementation of the shallow water equations, I wrote the program myself, verification is required. I verified my model with unit tests and an animation of a wave propagating.

In the shallow water model, waves propagate at approximately the square root of the product of gravity and depth. I let a wave propagate out for a fixed amount of time in simplified/controlled

conditions. I then compared the distance it went divided by the time it took with the expected approximate square root gravity times depth value. See figure 8.

I also verified my model by showing a simple initial disturbance propagate outwards in all directions within simplified/controlled conditions. See figure 7. This shows the model is working as expected and produces what one would expect to see in these conditions.



4 Results

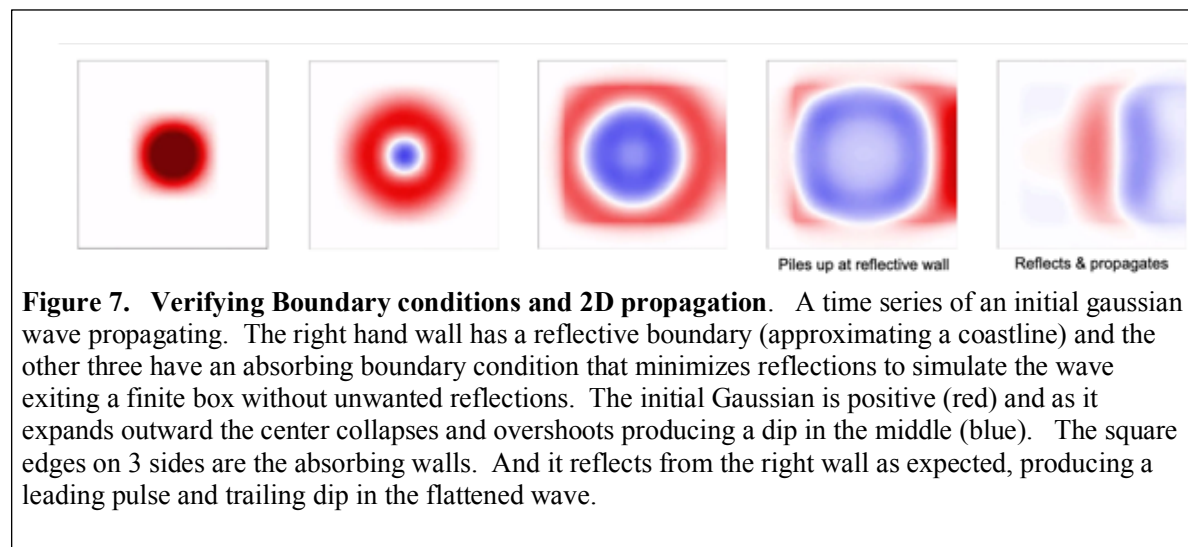
Palu

A Time series of the wave propagating is shown in figure 11. The wave starts as a simple initial disturbance and then propagates out into a ring. The wave flattens against the coast. A part of the wave enters Palu bay, and propagates down to the end. The wave on the heat map reddens upon reaching the end of the bay, indicating it is increasing in height as it strikes Palu city.

I ran many simulations varying the origin location of the tsunami, the height of the tsunami, and three different tsunami wave shapes in various orientations. I compared the maximum wave heights in Palu bay resulting from each one. A subset of these many runs are shown in figure 12abc. I have only shown 3 types of Tsunami wave shapes here because overall the results are similar in their forecast of where the wave will strike, meaning that the initial tsunami wave shape is not a major factor in the outcome at a distant location.

In each plot the initial condition of each event is displayed, beside the resulting maximum water height in Palu. The maximum water height contains the largest height a point reached during the whole simulation, for each point. This is displayed as an image. The impact of the tsunami at a given location is expected to correlate to the maximum water heights near that location, and so maximum height is used as a measure of impact. (Kristina, W)

The location of the origin, and bathymetry visibly affect the Maximum Wave Heights in figure 12abc. And the bathymetry dramatically affects the wave height as seen in the time series Figure 11.



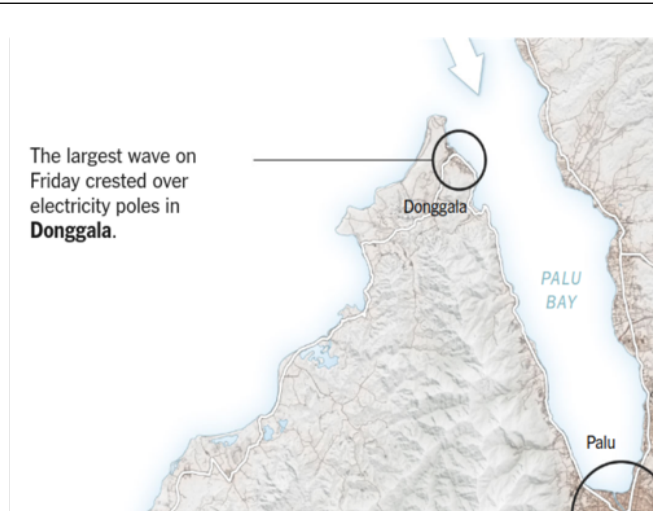


Figure 9: (NY Times) image of Palu Bay. The largest waves were recorded on the left side of the entrance to the bay. Palu City was the next highest wave height observed.

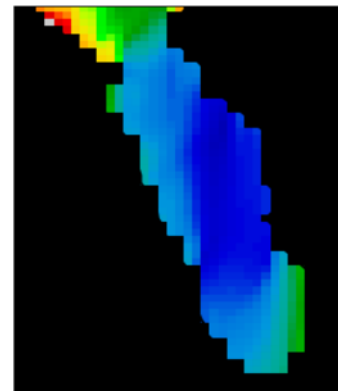


Figure 10: Palu bay maximum wave heights from simulation of actual event. Heatmap image shows highest waves were at the entrance to Palu bay. The particular simulation shows the results for a elliptical gaussian. Tsunami shape. Results for other Tsunami shape models are similar and show in figures below.

Animation of a Tsunami simulation starting North of Palu bay

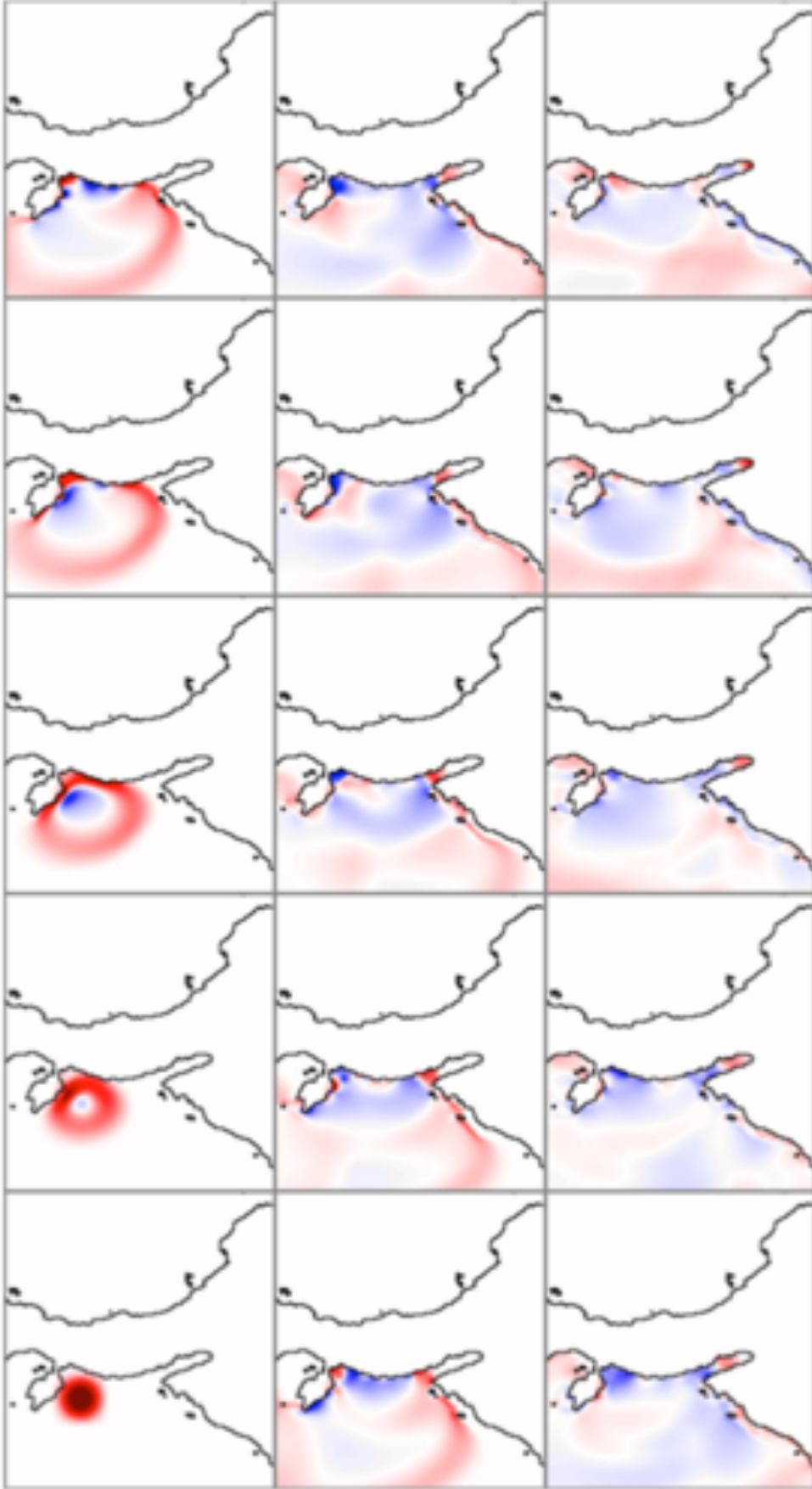


Figure 11. Time series of the Tsunami wave height at 100 second intervals. RED: positive wave height, BLUE negative, BLACK coast. The wave noticeably bends as it nears the shallow water near the coast. Palu bay is the notch in the lower middle of the image. Notice the Red brightens as it enters the harbor. This corresponds to the observed high wave in reality. The wave speed increases in the deep harbor water. Then the Red brightens again as it reaches the shallow slope at the end of the Palu bay where the city is located

Krakatoa

The maximum heights from the simulation of the Krakatoa case are seen in figure 14. A map showing where damage was inflicted on the surrounding coast in real life is seen in figure 13. These are compared as a measure of the accuracy of the simulation to real life. If the simulation produces larger maximum heights at areas that suffered a lot of damage in real life and produces smaller maximum heights at areas that suffered little damage in real life, then the model is accurate to real life. As it is compared, the model is found to be very similar to the real life damage map, and so very accurate.

Computer Model

The computer model was continuously produced during this project. It was over a thousand lines of code in total. Much more than just a shallow water computer model was created. In this project, big data was handled, an interactive graphical user interface was created, and code was written in multiple different ways, allowing for vector operations and running the code on a massive scale with thousands of parallel threads. Bathymetry data was acquired for all over the globe, meaning the model can easily be applied to anywhere on Earth. Additionally, the model simulates many times faster than real time, meaning given an initial tsunami, the model can accurately predict what it will do before the real tsunami does it.

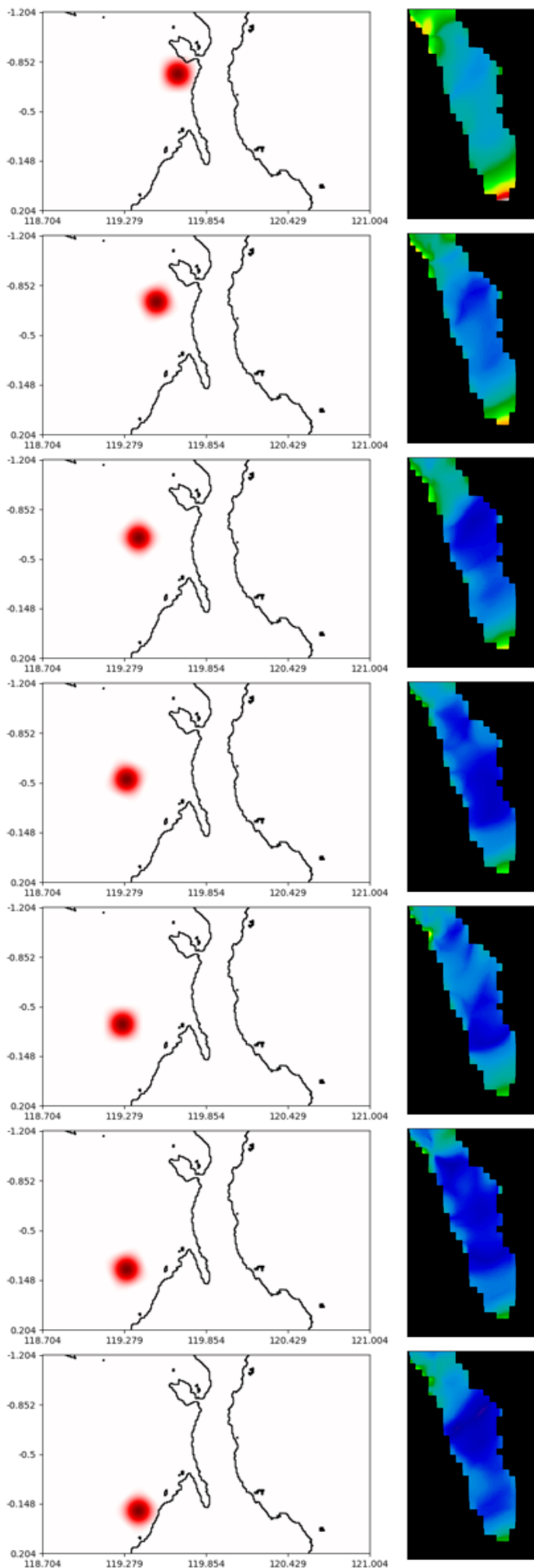


Figure 12a: a 5 meter tall round gaussian wave.

Simulations were run using different wave shapes, orientations, and heights. A sample of three of these are shown in Figure 7.

Figure 7a shows a 5 meter tall round gaussian wave.

LEFT: the initial condition,

RIGHT: the resulting maximum water height in Palu bay.

Observations:

1. **Alignment:** Only when the northern most events must align with the bay axis in a very narrow angle are high waves produced in Palu.
2. **Bay shape:** The largest waves occur at the base of the cove and at the very entrance.

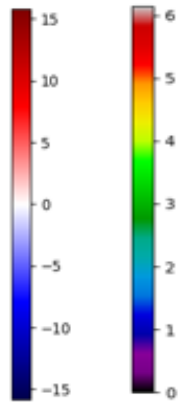
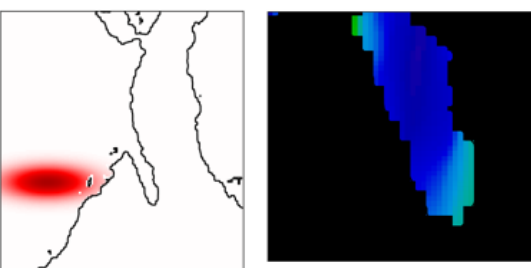
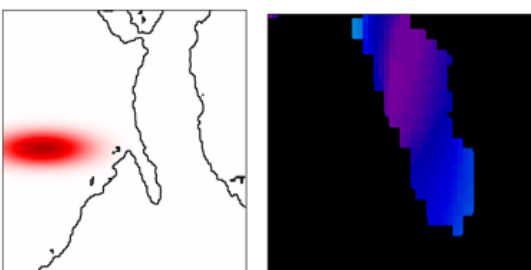
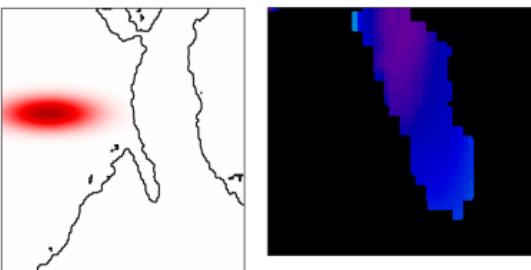
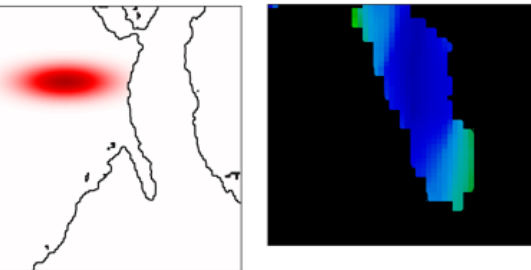
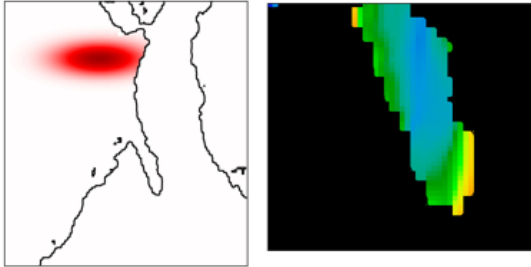
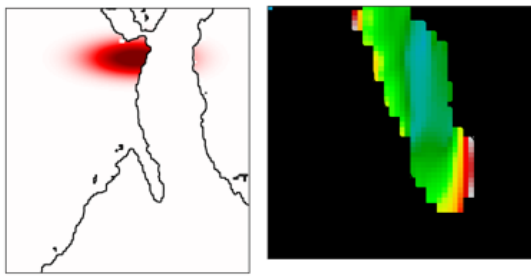


Figure 12b: a 15 meter tall, wide, elliptical gaussian in a particular orientation relative to Earth

Simulations were run using different wave shapes, orientations, and heights. Only three of these are shown in this report as they were generally similar.

This series uses a more intense elongated ellipse. The greater intensity appears to be responsible for the added observation of the kelvin wave.

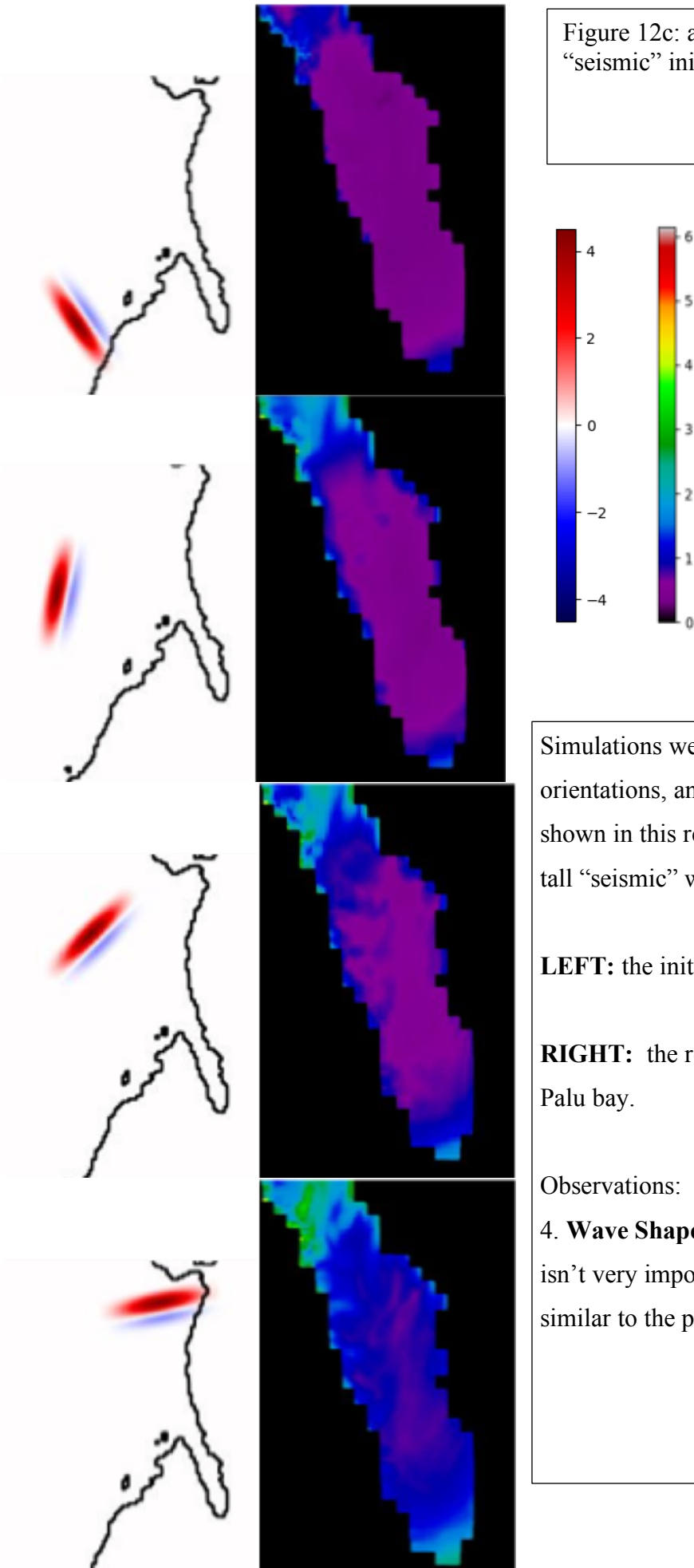
LEFT: the initial condition,

RIGHT: the resulting maximum water height in Palu bay.

Additional Observations:

3. **Kelvin Wave:** While overall, less aligned events couple less energy into the bay, surprisingly, the southern most event (bottom) shows an increase in the amount of wave height coupling into the bay compared to more northern waves

Figure 12c: a 15 meter tall, wide, “seismic” initial condition



Simulations were run using different wave shapes, orientations, and heights Only three of these are shown in this report Figure 12c shows a 5 meter tall “seismic” wave.

LEFT: the initial condition,

RIGHT: the resulting maximum water height in Palu bay.

Observations:

4. **Wave Shape:** Evidently the initial wave shape isn't very important to the outcome as this is similar to the previous two.

5 Discussion

Palu

Figure 12 displays data from multiple type of initial condition. The first is a circular gaussian, the most simple of initial conditions. The next is an elliptical gaussian, which may make more sense because an earthquake fault will be long in one dimension. Then, there is the “seismic” condition, which is much more realistic for an earthquake or slip fault source event. This initial condition is composed of two elliptical gaussians, one positive and one negative. The following is true for all of these.

Did the harbor shape or bathymetry have an effect?

In figure 11, deeper red represents higher waves, and deeper blue represents more negative waves. As the wave propagates out from its starting point, it is most red at the South side, which is the piece of the wave that will enter Palu Bay. The wave is very red as it enters Palu bay, but then much fainter as it goes down Palu bay. It then gets much redder at the end of Palu Bay, right at Palu city. This is because the end of the bay is shallower, so the wave is pushed up higher. Yes, the harbor shape and bathymetry had an effect.

Did the tsunami’s initial location have an effect?

Multiple simulations are represented in each section of figure 12 (12a, 12b, 12c). On the left, the initial condition is shown, and on the right, the resulting maximum height in Palu Bay is shown. More warm colors such as red and yellow represent higher waves, while cooler colors such as blue and purple represent lower waves. The image with the most “warm” colors in it is the maximum height plot corresponding to the initial condition in which the tsunami starts most North. Initial conditions South of the angle of Palu Bay have much “cooler” maximum height graphs. The intensity appears to drop off significantly as the initial tsunamis passes the angle of Palu bay. Tsunamis starting South of a line extended from Palu through the mouth of Palu bay do much less damage. Yes, the tsunami’s initial location had an effect.

Did the properties of the wave have an effect?

All the initial conditions or wave types tested displayed similar results, with one small exception. Only true of the elliptical initial condition, the intensity increases again in the final data point. This is likely because of a Kelvin wave (“Kelvin Waves.”), a wave that is guided along the coast. This tsunami starts close to the coast, so a Kelvin wave is likely, and may guide the wave up to the mouth of Palu bay. Because the Coriolis force is asymmetric this not seen in waves reflected off the north wall in the animation. For the most part, no, the properties of the wave did not have an effect.

Even larger maximum wave heights were observed at the mouth of Palu bay. This agrees with the real case, in which the highest waves were seen exactly. The model forecasted relatively lower wave heights along the inlet only becoming high again as it approached Palu, agreeing with reports. This shows that the forecast not only predicts where the waves will be high waves but it predicts where they are low

too. See figures 9 and 10. Because these observations agree, this point serves as further validation for my model.

For forecasting purposes some factors suggested by experts did not matter. The height of the tsunami, the shape of the tsunami, and the orientation of the tsunami did not strongly affect where the highest waves occurred. The kelvin wave effect is seen more clearly in the larger tsunamis but is visible in both the high and low wave height examples shown in the figures. Thus, Palu's unfortunate devastation was a matter of the bathymetry profile and the very unlucky location of the event being in exactly the worst possible place.

Krakatoa

Between figures 13 and 14, showing the maximum water heights produced by my simulation, and figure 13, a map displaying what areas were affected most in the real event, many similarities can be seen. Darker shades of red on the maximum water height images are located similarly to patches of yellow in the affected areas map and lighter shades of red located near the blank patches on the map, meaning the simulation produced similar results to that seen in real life. No factors were controlled to make the model fit real life better, meaning this model is run in a forecasting mode, rather than a model fitting mode. This means the model could be used as a danger forecaster to predict what regions of an area will be most severely damaged by a tsunami, with a high degree of accuracy.

Again, the forecast of both high and low threat areas is shown to agree with the news reports of damage. Notice in figures 13 and 14 that the Pesawaran and Sunda strait near Serang and Pagelaran coasts escaped inundation, as the predictions also indicate. This is despite appearing to be in line of sight with the tsunami origin, thus safe zones are not necessarily obvious ahead of time. Likewise, damage is seen wrapping around to behind the coast, so obvious safe zones may not be safe. It is important that both safe zones and hazard areas were predicted, because people need to know where to flee to, and where not to flee from.

Volcano-triggered tsunami hits Indonesia

The powerful tsunami struck at night and without warning, sweeping over popular beaches and inundating tourist hotels and coastal settlements

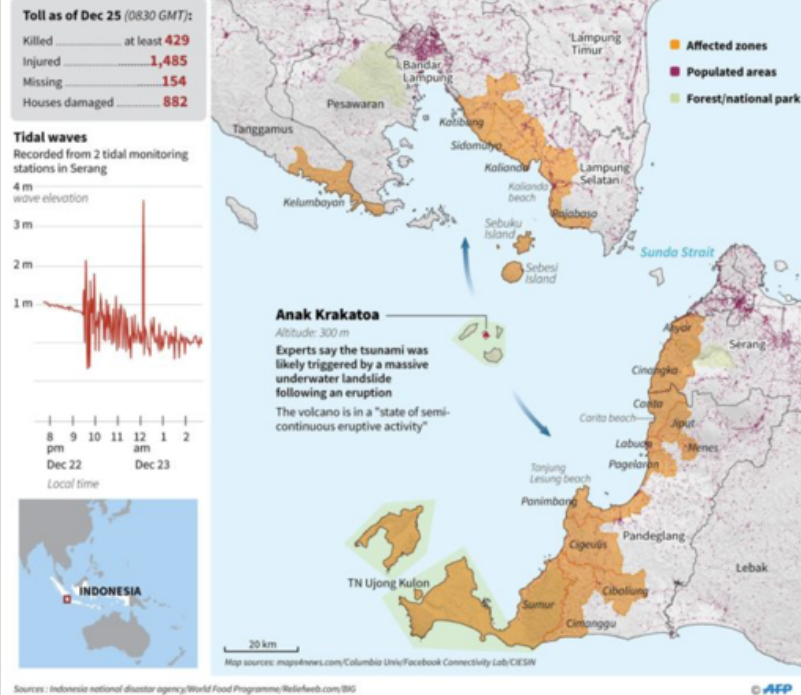


Figure 13: (Singapore news) Map of effected areas from Krakatoa tsunami. Orange colored regions represent flooded areas, and blank areas are less effected. Notice that the Pesawaran and Sunda strait near Serang and Pagelaran coasts escaped inundation, as the predictions also indicate.

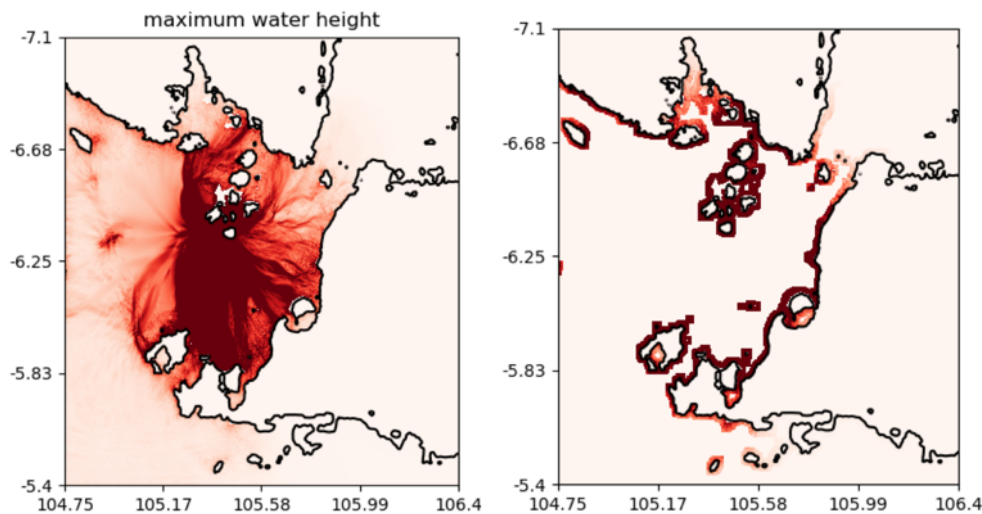


Figure 14: The Krakatoa Forecast: maximum water heights produced by the computer simulation. Some areas are much more effected, visualized by being a deeper red. The distribution of high waves along the coast varies considerably. For better visibility near the coast, the color bar is clipped at the high end **Left plot:** shows only the intensity near shore. Axes are Latitude and Longitude.

6 Conclusion

It was found that the shape of Palu bay did indeed worsen the Palu tsunami. I successfully created my own finite element implementation of the shallow water equations. My findings for the Palu case show: First, as one might guess, narrow inlets are protective in that they limit the directions from which a tsunami can easily enter. Second, the inlet's tapering ocean floor will also guide and amplify waves that do enter as they reach the end of the bay. And third, most surprisingly, special coastal features outside of the inlet can unexpectedly expand the hazard zone, via a Kelvin wave traveling along the southern side of the bay.

A pleasantly surprisingly high degree of accuracy was found for risk assessment of the Krakatoa case. Not only does it predict all the observed high water inundations but it also predicts where they did not happen. This shows the model would be excellent for risk forecasting, something that could save lives by predicting tsunami danger zones. This model could be used in the future to create a danger level map of a whole region, which could determine what regions are at especially high risk, and so what regions should take precaution.

The constructed computer model was able to simulate much faster than real time, and can be applied for any location on Earth. In the future it could form the basis for an integrated seismic event warning system if it were coupled with real time seismometer event locations. Because it runs faster than real-time on an inexpensive GPU it could be affordable to businesses and villages in seismically active regions.

The code is documented and available on Git Hub at this link:
<http://github.com/robertstrauss/shallowwater>.

7 Acknowledgements

LD created the on-line web site report. RRS wrote the code, designed and performed the experiments, and wrote the report and poster. Mentor MP suggested the shallow water equations, provided literature and tutorials on integration of the equations, and made suggestions for organizing the poster. Mentor CEMS taught python suggested key libraries like pandas, numba and numpy, how to code and reviewed the code for errors and bugs. Bill Lucy Knight, University of Alaska provided some hints on the shallow water equations by e-mail.

8 References

1. Caminha, Guilherme. “The CFL Condition and How to Choose Ymy Timestep Size.” *SimScale*, SimScale, 21 Mar. 2019, www.simscale.com/blog/2017/08/cfl-condition/
2. Center, National Geophysical Data. Tsunami Events Full Search, Sort by Date, Country. https://www.ngdc.noaa.gov/nndc/struts/results?bt_0=&st_0=&type_8=EXACT&query_8=None+Selected&op_14=eq&v_14=&st_1=&bt_2=&st_2=&bt_1=&bt_10=&st_10=&ge_9=&le_9=&bt_3=&st_3=&type_19=EXACT&query_19=74&op_17=eq&v_17=&bt_20=&st_20=&bt_13=&st_13=&bt_16=&st_16=&bt_6=&st_6=&ge_21=&le_21=&bt_11=&st_11=&ge_22=&le_22=&d=7&t=101650&s=70. Accessed 16 Dec. 2018.
3. Coastal National Elevation Database (CoNED) Project - Topobathymetric Digital Elevation Model (TBDEM) | The Long Term Archive. https://lta.cr.usgs.gov/coned_tbdem. Accessed 6 Dec. 2018.
4. “Indonesia Tsunami Kills Hundreds after Krakatau Eruption.” *BBC News*, BBC, 23 Dec. 2018, www.bbc.com/news/world-asia-46663158.
5. Indonesia Tsunami Worsened by Shape of Palu Bay: Scientists. <https://www.yahoo.com/news/indonesia-tsunami-worsened-shape-palu-bay-scientists-025002225.html>. Accessed 16 Jan. 2019.
6. Kelvin Waves. www.oc.nps.edu/webmodules/ENSO/kelvin.html.
7. Kristina, W. Effective Coastal Boundary Conditions for Tsunami Simulations. 2014. ---. Effective Coastal Boundary Conditions for Tsunami Simulations. 2014.
8. Randall, David A. “The Shallow Water Equations.” Selected Papers, p. 11. Shallow.Pdf. <http://kestrel.nmt.edu/~raymond/classes/ph589/notes/shallow/shallow.pdf> . Accessed 6 Dec. 2018.
9. Synolakis, C. E., et al. “Validation and Verification of Tsunami Numerical Models.” *Pure and Applied Geophysics*, vol. 165, no. 11–12, Dec. 2008, pp. 2197–228. Crossref, doi:10.1007/s00024-004-0427-y. ---. “Validation and Verification of Tsunami Numerical Models.” *Tsunami Science Fmy Years after the 2004 Indian Ocean Tsunami: Part I: Modelling and Hazard Assessment*, edited by Phil R. Cummins et al., Birkhäuser Basel, 2009, pp. 2197–228. Springer Link, doi:10.1007/978-3-0346-0057-6_11.
10. Thacker, William Carlisle. “Some Exact Solutions to the Nonlinear Shallow-Water Wave Equations.” *Journal of Fluid Mechanics*, vol. 107, June 1981, pp. 499–508. Cambridge Core, doi:10.1017/S0022112081001882.
11. Time-Stepping Schemes Review - WikiROMS. https://www.myroms.org/wiki/Time-stepping_Schemes_Review#Forward-Backward_Feedback_.28RK2-FB.29. Accessed 6 Dec. 2018.
12. Tinti, S., and R. Tonini. *The UBO-TSUF D Tsunami Inundation Model: Validation and Application to a Tsunami Case Study Focused on the City of Catania, Italy*. 2013
13. Giachetti, T. ,Karim R., Budianto, K. Tsunami hazard related to a flank collapse of Anak Krakatau Volcano, Sunda Strait, Indonesia, January 2012 Geological Society London
14. Ontowirjo Smith, Nicola. “Indonesia Tsunami: At Least 222 Dead and 843 Injured after Anak Krakatau Volcano Erupts .” *The Telegraph*, Telegraph Media Group, 22 Dec. 2018, www.telegraph.co.uk/news/2018/12/22/indonesia-tsunami-least-20-dead-165-injured-waves-hit-beaches/.
15. Ali, Hani, et al. “APPLICATION OF THE SHALLOW WATER EQUATIONS TO REAL FLOODING CASE.” *Proceedings of the VII European Congress on Computational Methods in Applied Sciences and Engineering (ECCOMAS Congress 2016)*, Institute of Structural Analysis and Antiseismic Research School of Civil Engineering National Technical University of Athens (NTUA) Greece, 2016, pp. 735–49. Crossref, doi:10.7712/100016.1849.10225.